Original Article

Radiat Oncol J 2016;34(3):230-238
http://dx.doi.org/10.3857/roj.2016.01788
pISSN 2234-1900 · eISSN 2234-3156

ROJ Radiation Oncology Journal

Gold nanoparticles enhance anti-tumor effect of radiotherapy to hypoxic tumor

Mi Sun Kim, MD[1*], Eun-Jung Lee, PhD[1], Jae-Won Kim, MS[1], Ui Seok Chung, BS[2], Won-Gun Koh, PhD[2], Ki Chang Keum, MD, PhD[1], Woong Sub Koom, MD, PhD[1]

[1]Department of Radiation Oncology, Yonsei University College of Medicine, Seoul;
[2]Department of Chemical and Biomolecular Engineering, Yonsei University, Seoul, Korea

Purpose: Hypoxia can impair the therapeutic efficacy of radiotherapy (RT). Therefore, a new strategy is necessary for enhancing the response to RT. In this study, we investigated whether the combination of nanoparticles and RT is effective in eliminating the radioresistance of hypoxic tumors.

Materials and Methods: Gold nanoparticles (GNPs) consisting of a silica core with a gold shell were used. CT26 colon cancer mouse model was developed to study whether the combination of RT and GNPs reduced hypoxia-induced radioresistance. Hypoxia inducible factor-1α (HIF-1α) was used as a hypoxia marker. The 3-(4,5-dimethylthiazol-2-yl)-2,5-diphenyltetrazolium bromide (MTT) assay and terminal deoxynucleotidyl transferase dUTP nick end labeling (TUNEL) staining were conducted to evaluate cell death.

Results: Hypoxic tumor cells had an impaired response to RT. GNPs combined with RT enhanced anti-tumor effect in hypoxic tumor compared with RT alone. The combination of GNPs and RT decreased tumor cell viability compare to RT alone *in vitro*. Under hypoxia, tumors treated with GNPs + RT showed a higher response than that shown by tumors treated with RT alone. When a reactive oxygen species (ROS) scavenger was added, the enhanced antitumor effect of GNPs + RT was diminished.

Conclusion: In the present study, hypoxic tumors treated with GNPs + RT showed favorable responses, which might be attributable to the ROS production induced by GNPs + RT. Taken together, GNPs combined with RT seems to be potential modality for enhancing the response to RT in hypoxic tumors.

Keywords: Nanoparticle, Hypoxia, Radiotherapy

Introduction

New technologies in radiotherapy (RT) have been developed to overcome the low tolerance of normal tissue and achieve a high therapeutic ratio. For example, image-guided RT has been used to identify the exact tumor location and the relationship between the tumor and normal organs. Intensity-modulated RT was developed to deliver high doses of radiation precisely to the tumor location by using a stiff dose gradient. Despite the use of these technologically advanced methods, tumor responses are limited in cases of hypoxic tumors. Hypoxia is a key regulatory factor in tumor growth [1] and plays a crucial role in RT resistance [2]. Furthermore, RT can result in cycling of hypoxia in tumor regions [3]. After RT, the lack of oxygen reduces the production of reactive oxygen species (ROS), and ultimately prevents irreparable DNA damage from occurring in

Received 7 May 2016, Revised 13 July 2016, Accepted 2 August 2016.
Correspondence: Woong Sub Koom, MD, PhD, Department of Radiation Oncology, Yonsei University College of Medicine, 50-1 Yonsei-ro, Seodaemun-gu, Seoul 03722, Korea. Tel: +82-2-2228-8116, Fax: +82-2-312-9033, E-mail: mdgold@yuhs.ac
*Current affiliation: Department of Radiation Oncology, CHA Bundang Medical Center, CHA University, Seongnam, Korea

tumor cells, thereby preventing tumor cell death [4]. Hypoxia also leads to the up-regulation of hypoxia-inducible factor 1α (HIF-1α), which independently promotes radioresistance [5].

One of measures to overcome the limitations of RT is the use of nanoparticles in RT. Nanoparticles are utilized for various purposes in antitumor treatments, such as drug delivery [6,7], diagnosis [8,9], gene therapy [10], and RT [11]. When nanoparticles are combined with RT, absorbed radiation dose increases. In particular, the use of gold nanoparticle (GNPs) to enhance RT efficacy is well established [12,13]. GNPs can enhance RT efficacy owing to their high K-edge [14]. Studies have explained the enhancement of RT using GNPs in medical physics [15,16]. One of the reasons for the enhancement of RT efficacy when used in combination with GNPs is ROS production when GNPs are subjected to X-ray irradiation. This ROS generation differs depending on the composition, size, and potential of GNPs [17].

We hypothesized that increased ROS production due to GNPs combined with RT overcomes the limited effect of RT under hypoxic conditions. This study was aimed at investigating the enhancement of RT efficacy using GNPs and evaluating the potential for increasing RT efficacy under hypoxic conditions.

Materials and Methods

1. Reagents

HIF-1α antibody was purchased from Abcam (Cambridge, UK), and 3-(4,5-dimethylthiazol-2-yl)-2,5-diphenyltetrazolium bromide (MTT) was obtained from Sigma (St. Louis, MO, USA).

2. GNP synthesis

The GNPs used in this study consisted of a silica core with a gold shell. Silica nanoparticles (SNPs) were functionalized with 3-aminopropyl triethoxysilane to help attachment of gold seeds (1–2 nm). Gold seeds were deposited onto the SNPs. Further gold coverage of the SNPs was accomplished by the reduction of gold hydroxide by hydroxylamine hydrochloride on the SNP surface (Fig. 1A) [18].

3. Cell culture

Mouse CT26 colon cancer cells were used for all experiments. The cells were cultured in RPMI 1640 (Gibco, Carlsbad, CA, USA) supplemented with 10% fetal bovine serum (FBS) and 1% antibiotics and maintained at 37°C in a 5% CO_2 incubator. They were subcultured every 3–4 days to maintain exponential growth.

4. MTT assay

Mouse CT26 colon cancer cells (4×10^3 cells/well) were plated onto 96-well plates. After 24 hours, the cells were incubated with 2 μg/mL GNP for 24 hours at 37°C in a 5% CO_2 incubator. After incubation, the cells were washed with phosphate buffered saline (PBS) to remove excess GNPs. The effect of GNPs on cell viability was evaluated using the MTT assay at 24 hours after GNP exposure.

5. Apoptosis assay

For *in vitro* apoptosis assay, cells were treated GNP with 2 μg/mL for 24 hours, which was washed with new media followed by irradiation with 8 Gy. After incubation for 48 hours, cells were stained with FITC-annexin V (BD Biosciences, San Jose, CA, USA) and propidium iodide (PI; BD Biosciences) for 15 minutes. Apoptotic cells were evaluated by flow cytometry analyses using FACSVerse flow cytometer (BD Biosciences).

6. Effect of the combination of GNPs and RT on cell growth under hypoxic conditions

To investigate the synergistic effect of GNPs and RT on cell growth inhibition under hypoxic conditions in comparison with that of RT alone, 4×10^3 cells/well were incubated with 2 μg/mL GNP for 24 hours at 37°C in a 0.1% O_2, 5% CO_2, and balanced N_2, respectively. After incubation, the cells were washed with PBS to remove excess GNPs followed by 8 Gy irradiation. A single fraction of 8 Gy was delivered to the tumor cells by using a X-RAD 320 irradiator (Precision X-Ray, North Branford, CT, USA) and cell viability was evaluated using the MTT assay.

7. Terminal deoxynucleotidyl transferase dUTP nick end labeling (TUNEL) staining

The TUNEL assay was performed according to the manufacturer's instructions (Promega Co., Madison, WI, USA). Briefly, after deparaffinization and rehydration, tissue sections were incubated with proteinase K (20 μg/mL) for 15 minutes at 24°C and washed in PBS. The slides were incubated with a mixture of TdT enzyme and biotinylated nucleotide for 60 minutes at 37°C. After being washed in PBS, the slides were incubated with streptavidin-horseradish peroxidase (HRP) solution for 30 minutes at 24°C. To detect TUNEL-positive signals, the slides were incubated with a mixture of 3,3'-diaminobenzidine (DAB) substrate, chromogen, and hydrogen peroxide. The slides were then examined and the images were recorded using a microscope (Olympus BX53F; Olympus, Tokyo, Japan). Dark brown staining represented

http://dx.doi.org/10.3857/roj.2016.01788

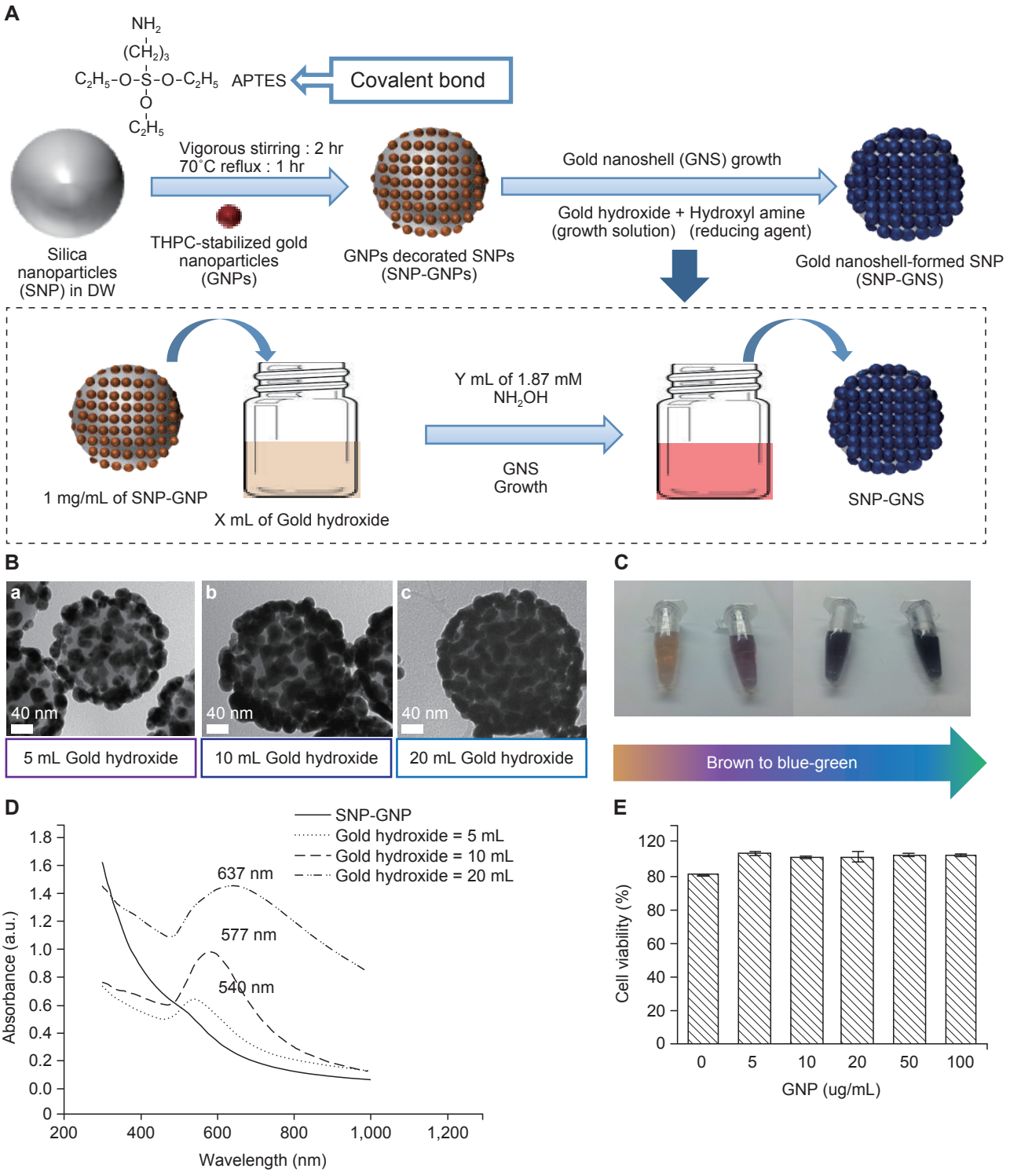

Fig. 1. Gold nanoparticle (GNP) characterization. (A) Schematic illustration of the synthesis of GNPs. (B) Transmission electron micrograph of gold shell formation in SNP-GNPs (SNP-GNS) with different amounts of gold hydroxide solution: (a) 5 mL, (b) 10 mL, and (c) 20 mL. (C) Color changes from SNP-GNP to SNP-GNS. (D) Absorption spectra of SNP-GNPs and SNP-GNS. (E) MTT viability assay of CT26 cells treated with increasing concentrations of GNPs for 24 hours. Cells were incubated with 2 μg/mL GNP for 24 hours and washed with new media to remove excess GNPs. Cell viability was evaluated using the MTT assay at 24 hours after GNP exposure. Error bars, viability (mean ± standard deviation of three replicates). All experiments were performed in triplicate. MTT, 3-(4,5-dimethylthiazol-2-yl)-2,5-diphenyltetrazolium bromide; APTES, 3-aminopropyltriethoxysilane; THPC, tetrakis (hydroxymethyl) phosphonium chloride.

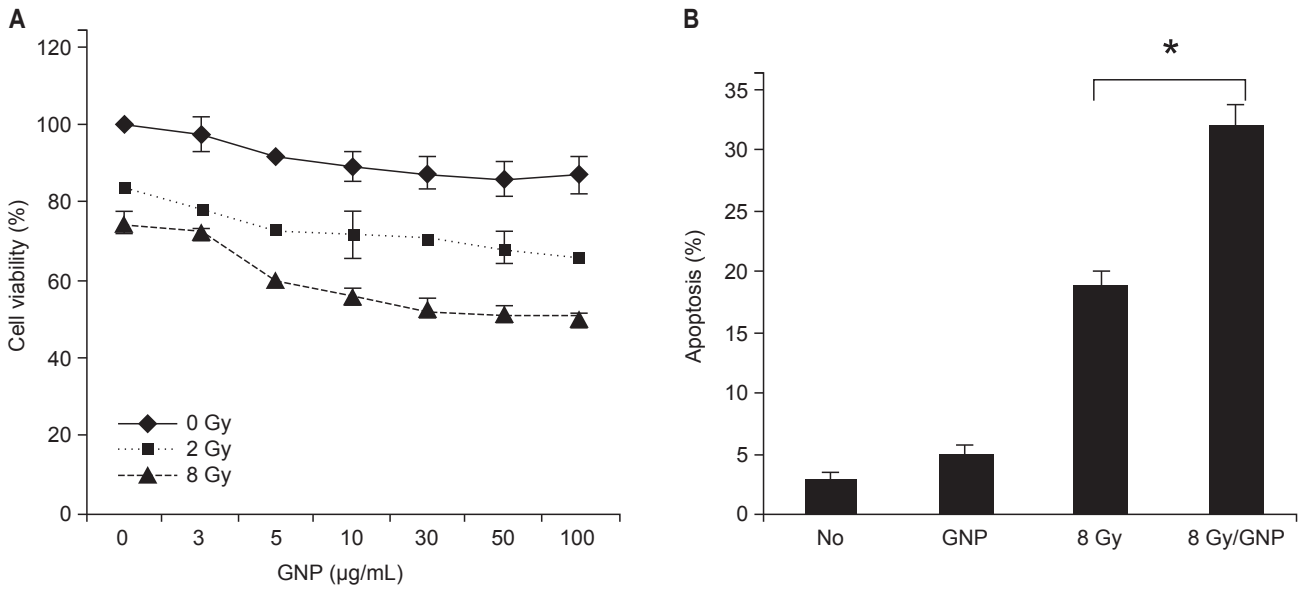

Fig. 2. Enhancement of radiosensitivity using gold nanoparticles. (A) MTT viability assay of CT26 cells after 2, 8 Gy irradiation at various concentration of gold nanoparticles (GNPs). CT26 cells were pre-treated with GNPs at various concentrations for 24 hours and irradiated after washing with new media. After 48 hours, cell viability was evaluated by MTT assay. (B) Apoptosis assay in CT26 cells treated with radiotherapy (RT) and GNPs + RT. CT26 cells were treated GNP with 2 μg/mL for 24 hours, followed by irradiation with 8 Gy after washing. Cells were stained with FITC-annexin V and propidium iodide for detection of apoptotic cells at 48 hours after irradiation. All experiments were performed in triplicate. MTT, 3-(4,5-dimethylthiazol-2-yl)-2,5-diphenyltetrazolium bromide. *$p < 0.05$.

a positive reaction. Positive reactions showed under the microscope, and stained cells were quantified by stereological analysis using Image-J software (https://imagej.nih.gov/ij/).

8. ROS evaluation

CT26 cells were cultured in a 6-well plate for 24 hours followed by 6 Gy irradiation. After incubation for 2 hours, the cells were treated with a fluorogenic probe, as an indicator, for ROS detection and measurements were performed using a fluorescence microscope (Zeiss, Jena, Germany). Dichlorodihydrofluorescein, supplied as a diacetate ester (DCFH DA), is readily oxidized to the highly fluorescent dichlorofluorescein (DCF) after enzymatic or base-catalyzed cleavage of the diacetate groups; 10 mM N-acetyl-L-cysteine (NAC) was used as a ROS scavenger.

9. Tumor growth inhibition (TGI)

The CT26 mouse colon cancer model was developed to investigate the synergistic effect of GNP in combination with RT on tumor growth. We injected 10^6 CT26 mouse colon cancer cells into the thigh of BALB/c mice subcutaneously. When tumor diameter reached 6 mm or 12 mm, GNPs (100 μg Au) were injected into tumors; thereafter, the tumors were irradiated with 10 Gy in a single fraction by using X-RAD 320 irradiator (Precision X-Ray). The mice were placed at a distance of 69 cm from the radiation source and treated at a dose rate of 150 cGy/min with 300 kVp X-rays, using 12.5 mA and a X-ray beam filter consisting of 2.0 mm Al. Tumor volume was calculated using the formula $0.5 \times ab^2$, where a is the long axis and b is the short axis of two orthogonal diameters. The mice were divided into the following 4 groups (A, control; B, GNPs; C, RT; D, GNPs + RT). Tumor growth delay was observed for 18 days.

10. Immunofluorescence staining for HIF-1α detection

Twenty four hours after irradiation, mice were sacrificed. Tumors were fixed in 4% paraformaldehyde and embedded in paraffin. The blocks were cut into 5-μm-thick sections. Antigen retrieval was accomplished at 37°C with protease K solution. For immunofluorescence staining, deparaffinized sections were blocked with 10% normal horse serum for 1 hour and then incubated with primary antibodies against HIF-1α for overnight at 4°C (Abcam). After washing with PBS, the samples were incubated for 1 hour with a PE conjugated secondary antibody (Thermo Fisher Scientific, Waltham, MA, USA). Reactions showed under the fluorescence microscope, and HIF-1α stained cells were quantified using Image-J software.

http://dx.doi.org/10.3857/roj.2016.01788

11. Statistical analysis

Tumor cell growth was compared using the Student t-test, and tumor growth was compared using repeated-measures ANOVA. A p-value less than 0.05 was considered statistically significant. All statistical analyses were performed using SPSS ver. 20.0 (IBM, Armonk, NY, USA).

Results

1. GNP characterization

The GNPs were imaged using transmission electron microscopy (Fig. 1B). The formation of GNPs was first confirmed by the color of the nanoparticle-containing solution. As further

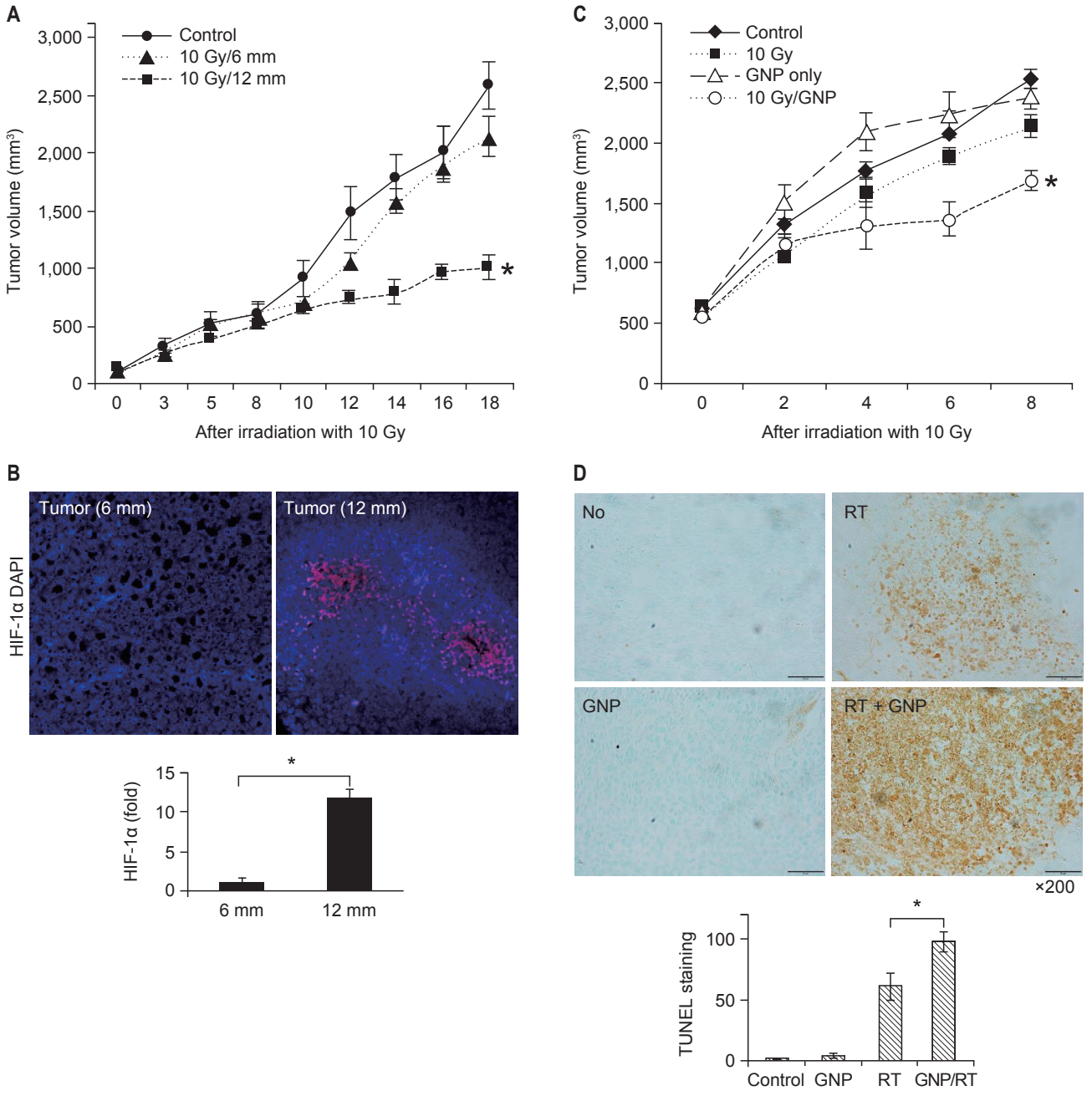

Fig. 3. Effect of hypoxia on tumor growth inhibition. (A) Tumor volume after 10 Gy irradiation in a single fraction. (B) Immunohistochemical staining for hypoxia inducible factor-1α (HIF-1α) in tumors with different diameters. (C) Tumor volume in 4 groups of mice after treatment. (D) Terminal deoxynucleotidyl transferase dUTP nick end labeling (TUNEL) staining of tumors in 4 groups of mice after treatment. All experiments were performed in triplicate. GNP, gold nanoparticle; RT, radiotherapy; DAPI, 4',6-diamidino-2-phenylindole. *$p < 0.05$.

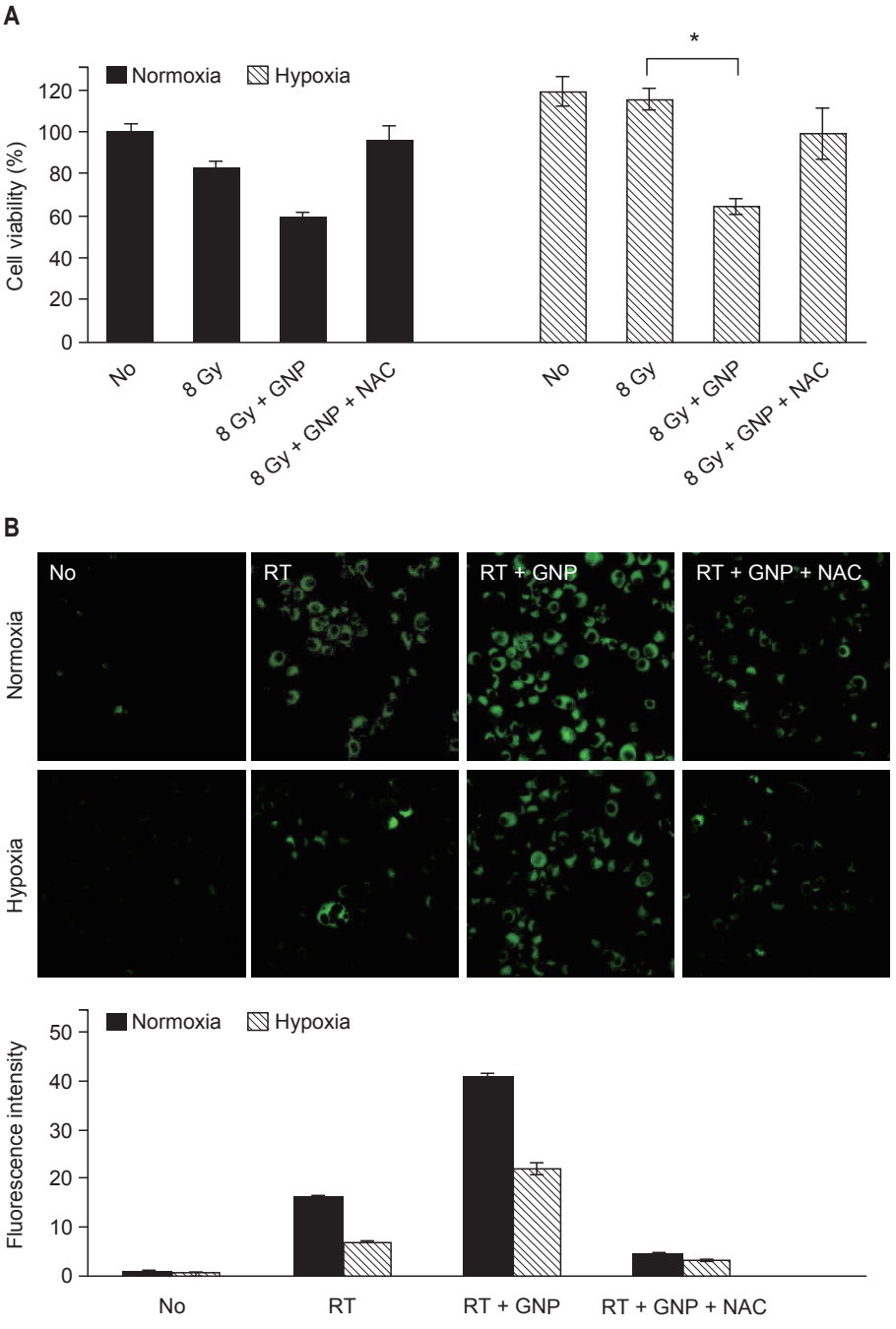

Fig. 4. Reactive oxygen species (ROS) evaluation. (A) MTT viability assays of CT26 cells after treatment under normoxic and hypoxic conditions. Error bars, viability (mean ± standard deviation of six replicates). (B) Relative ROS generation in CT26 cells after treatment under normoxic and hypoxic conditions. All experiments were performed in triplicate. MTT, 3-(4,5-dimethylthiazol-2-yl)-2,5-diphenyltetrazolium bromide; GNP, gold nanoparticle; NAC, N-acetyl-L-cysteine; RT, radiotherapy. *$p < 0.05$.

gold coverage was achieved, the color of the GNP-containing solution changed from brown to blue-green (Fig. 1C), and the absorbance peak of the solution widened and red-shifted (Fig. 1D). After addition of 0.250 mM gold hydroxide, a fairly thick GNP was obtained. The mean diameter of the GNPs was 180 nm. The resultant GNPs exhibited a small absorbance peak at 540 nm [18]. The cytotoxicity of GNPs was evaluated using the MTT assay. GNPs did not affect cell viability until 100 μg/mL (Fig. 1E).

2. GNPs enhanced the radiosensitivity of tumor cells

To investigate synergistic effect of GNPs used in combination with RT on TGI, CT26 cells were treated with GNPs in the absence or presence of radiation. After administration of 2, 8 Gy in a single fraction to CT26 tumor cells, a dose-response relationship was observed at various concentrations of GNPs (Fig. 2A). Tumor cells treated with 8 Gy showed less survival than that shown by the cells treated with 2 Gy. As the concentration of the GNPs increased, cell viability slightly

http://dx.doi.org/10.3857/roj.2016.01788

decreased.

GNPs combined with RT increased apoptosis significantly (Fig. 2B). In comparison with cells treated with RT alone, those treated with GNPs + RT showed significantly greater apoptosis.

3. Synergistic effect of GNPs in combination with RT on TGI in hypoxia

To evaluate the effect of hypoxia on TGI, tumors with different diameters after treatment with 10 Gy in a single fraction were compared (Fig. 3A). While the tumor with a diameter of 6 mm showed significant TGI after irradiation, the tumor with a diameter of 12 mm did not show significant TGI. Immunohistochemical staining for HIF-1α showed that tumor with the diameter of 12 mm had more hypoxic tumor cells (Fig. 3B).

To evaluate the synergistic effect of GNPs in combination with RT under hypoxic conditions, tumor volumes of the mice in the 4 groups (A, B, C, and D) were compared (Fig. 3C). Group D (GNPs + RT) showed better TGI than that shown by group C (RT). During the follow-up period, groups A-C showed no difference in tumor volume. Apoptosis after irradiation was investigated using TUNEL staining. The number of TUNEL-positive cells increased in group D compared to those in groups A-C (Fig. 3D).

4. GNP induced ROS-dependent apoptosis

To investigate the mechanism of the synergistic effect of GNPs combined with RT, cell viability was compared using the MTT assay (Fig. 4A). Under normoxic conditions, GNPs combined with RT showed an enhanced antitumor effect on tumor cells. Tumor cells treated with GNPs + RT had lower survival than those treated with RT alone. Meanwhile, the improved antitumor effect diminished when NAC added. Under hypoxic conditions, the enhancement of the effect of RT due to GNPs was more notable. The effect of RT on cell viability under hypoxic conditions was slight. GNPs combined with RT showed a synergistic effect and the survival of the cells treated with GNPs + RT was significantly lower than that of the cells treated with RT alone.

ROS generation was observed using a fluorogenic probe (Fig. 4B). Under normoxic conditions, ROS generation was detected in cells treated with RT. The fluorescence intensity increased significantly in the cells treated with GNPs + RT. Fluorescence intensity decreased upon addition of NAC, and the same patterns were observed under hypoxic conditions. The antitumor effect of GNPs + RT was correlated with ROS generation. When ROS generation increased, the survival of cells decreased. When ROS was removed using NAC, the survival of cells recovered.

Discussion and Conclusion

Oxygen is well-established radiosensitizer. Free radicals generated after irradiation break the DNA double strand and induce biological damage in tumors. Oxygen fixes DNA damage, resulting in enhancement of RT efficacy [19]. Therefore, the oxygen effect is limited under hypoxic conditions.

Tumor cells often are under hypoxic conditions. In particular, in large tumors, some tumor cells are located far from blood vessels. Tumor blood vessels are immature, and therefore, temporary obstruction occurs often. Hypoxic conditions affects both the DNA damage repair pathway and cell survival signaling pathway [20]. HIF-1α becomes activated in hypoxic conditions, and results in increased expression of genes related to angiogenesis, invasion and metastasis of tumor cells [3].

We observed that hypoxic tumor cells had an impaired response to RT. GNPs combined with RT enhanced the antitumor effect in hypoxic tumor cells. After irradiation, the survival of hypoxic tumor cells was higher than that of normoxic tumor cells. Addition of GNPs decreased tumor cell viability significantly. The tumor growth was impaired in both small tumor and large tumors after administration of 10 Gy in a single fraction. However, large tumors, which had more hypoxic tumor cells, showed a poor response. When we evaluated tumor growth after the administration of 10 Gy in a single fraction, the tumors treated with GNPs + RT showed a higher response than that shown by the tumors treated with RT alone. With regard to tumor cell death, the cells treated with GNPs + RT and NAC showed a higher survival rate than that shown by the cells that were not treated with NAC. Apoptosis due to ROS was one of the main mechanisms of cell death.

In clinical practice, stereotactic body radiotherapy (SBRT) is used to overcome the radioresistance of hypoxic tumors [21]. SBRT delivers an ablative radiation dose to the tumor area in 1–5 fractions. However, stereotactic radiosurgery and SBRT with the current doses cannot directly kill all the hypoxic cells in the tumor. GNPs when combined with RT enhance RT efficacy. Gold has a high atomic number. It is advantageous to interact with KeV energy radiation (photoelectric effect). Due to the photoelectric effect, short-range photo-Auger electrons emitted from the GNPs boost the tumor area while sparing the adjacent normal tissue.

Some studies pointed out the discrepancy between

predicted dose enhancement via a photoelectric effect and the radiobiological response of GNPs combined with RT [22,23]. Butterworth and colleagues focused on ROS. GNPs combined with RT elicit tumor cell responses mediated through oxidative stress. They suggested that oxidative stress via ROS is one of the main mechanisms of tumor response. GNPs contribute to increased ROS production when a tumor is irradiated. Misawa and colleagues studied the factors that affected ROS generation in the presence of GNPs [24]. The Auger electron and fluorescent X-ray, which were the resultants of interaction of ionizing radiation with GNPs, cause secondary water radiolysis. In addition to primary water radiolysis, secondary water radiolysis can produce additional ROS. Our study also showed increased ROS generation upon using GNPs. We used a cell-permeable fluorogenic probe to detect the presence of ROS. Tumor cells treated with GNPs + RT showed increased ROS generation.

GNPs in combination with RT induce decreased clonogenic cell survival, increased apoptosis, and DNA damage [23], which are related to oxidative stress. Therefore, GNPs combined with RT may synergistically cause radiochemical damage via ROS [24]. In the present study, tumor cells treated with GNPs + RT exhibited increased apoptosis. It was correlated with ROS generation. In hypoxic conditions, GNPs enhanced RT efficacy. The viability of tumor cells decreased significantly when treated with GNPs + RT. However, the effect was diminished when a ROS scavenger was added.

GNPs combined with RT may have boost effect to tumor area. Berbeco et al. [16] reported a boosting dose for tumor endothelial cells using megavoltage X-rays. They showed local dose enhancement for the tumor microvasculature by using linear accelerator X-ray. They found that GNPs combined with external-beam RT could deliver a prescribed dose to tumor cells and boost dose to the tumor microvasculature concomitantly. Tumors with disrupted microvasculature are deficient in nutrients and oxygen, which leads to necrosis. Rapid intratumoral necrosis results in remnant viable tumor cells around the margin of the necrotic area. The remnant viable tumor cells are close to normal tissue vasculature, and could be re-oxygenated, making them good targets for RT [25]. In our study, tumors treated with GNPs + RT showed better responses than those treated with RT alone during the follow-up period. After administration of a single fraction of radiation, remnant viable tumor cells close to the normal vasculature might be re-oxygenated, and the oxygen effect might induce increased tumor cell death.

This study was insufficient to gather robust evidence for the enhancement of RT efficacy by GNPs to overcome hypoxia. GNPs were administered by intratumoral injection, and we could not be sure that they were distributed evenly in the tumor. The absorbed dose was not measurable. It could be odd that tumors with 12 mm diameter were defined as hypoxic tumors based on HIF-1α immunohistochemistry staining. Tumors in different size may have different characteristics. Furthermore, hypoxia is not the only factor that can influence on radiation sensitivity. In future studies, we should follow a way to make hypoxic tumor with similar size as a previous work [26].

Finally, in this study, GNPs combined with RT exhibited a favorable response in hypoxic tumors, which were resistant to RT. RT administered with high-tech therapeutic machinery alone has not shown a favorable effect in hypoxic tumors and tolerability in normal tissues, simultaneously. However, GNPs combined with RT enhanced ROS generation in hypoxic tumors, leading to tumor cell apoptosis. Thus, GNPs combined with RT may have potential for enhance the efficacy of RT. We expect further studies on clinical application of GNPs combined with RT.

Conflict of Interest

No potential conflict of interest relevant to this article was reported.

Acknowledgments

This work was supported by the Korean Society for Radiation Oncology (KOSRO) Young Investigator Fund.

References

1. Harris AL. Hypoxia: a key regulatory factor in tumour growth. Nat Rev Cancer 2002;2:38-47.
2. Overgaard J. Hypoxic modification of radiotherapy in squamous cell carcinoma of the head and neck: a systematic review and meta-analysis. Radiother Oncol 2011;100:22-32.
3. Harada H. How can we overcome tumor hypoxia in radiation therapy? J Radiat Res 2011;52:545-56.
4. Barker HE, Paget JT, Khan AA, Harrington KJ. The tumour microenvironment after radiotherapy: mechanisms of resistance and recurrence. Nat Rev Cancer 2015;15:409-25.
5. Semenza GL. Intratumoral hypoxia, radiation resistance, and HIF-1. Cancer Cell 2004;5:405-6.
6. Han G, Ghosh P, Rotello VM. Functionalized gold nanoparticles for drug delivery. Nanomedicine (Lond) 2007;2:113-23.

http://dx.doi.org/10.3857/roj.2016.01788

7. Zhao Y, Yu B, Hu H, Hu Y, Zhao NN, Xu FJ. New low molecular weight polycation-based nanoparticles for effective codelivery of pDNA and drug. ACS Appl Mater Interfaces 2014;6:17911-9.
8. Qian X, Peng XH, Ansari DO, et al. In vivo tumor targeting and spectroscopic detection with surface-enhanced Raman nanoparticle tags. Nat Biotechnol 2008;26:83-90.
9. Perrault SD, Walkey C, Jennings T, Fischer HC, Chan WC. Mediating tumor targeting efficiency of nanoparticles through design. Nano Lett 2009;9:1909-15.
10. Conde J, Rosa J, de la Fuente JM, Baptista PV. Gold-nanobeacons for simultaneous gene specific silencing and intracellular tracking of the silencing events. Biomaterials 2013;34:2516-23.
11. Hainfeld JF, Slatkin DN, Smilowitz HM. The use of gold nanoparticles to enhance radiotherapy in mice. Phys Med Biol 2004;49:N309-15.
12. Roeske JC, Nunez L, Hoggarth M, Labay E, Weichselbaum RR. Characterization of the theorectical radiation dose enhancement from nanoparticles. Technol Cancer Res Treat 2007;6:395-401.
13. Cho SH, Jones BL, Krishnan S. The dosimetric feasibility of gold nanoparticle-aided radiation therapy (GNRT) via brachytherapy using low-energy gamma-/x-ray sources. Phys Med Biol 2009;54:4889-905.
14. Rahman WN, Bishara N, Ackerly T, et al. Enhancement of radiation effects by gold nanoparticles for superficial radiation therapy. Nanomedicine 2009;5:136-42.
15. Kojima C, Hirano Y, Yuba E, Harada A, Kono K. Preparation and characterization of complexes of liposomes with gold nanoparticles. Colloids Surf B Biointerfaces 2008;66:246-52.
16. Berbeco RI, Ngwa W, Makrigiorgos GM. Localized dose enhancement to tumor blood vessel endothelial cells via megavoltage X-rays and targeted gold nanoparticles: new potential for external beam radiotherapy. Int J Radiat Oncol Biol Phys 2011;81:270-6.
17. Retif P, Pinel S, Toussaint M, et al. Nanoparticles for radiation therapy enhancement: the key parameters. Theranostics 2015;5:1030-44.
18. Chung US, Kim JH, Kim B, Kim E, Jang WD, Koh WG. Dendrimer porphyrin-coated gold nanoshells for the synergistic combination of photodynamic and photothermal therapy. Chem Commun (Camb) 2016;52:1258-61.
19. Hall EJ, Giaccia AJ. Oxygen effect and reoxygenation. In: Hall EJ, Giaccia AJ, editors. Radiobiology for the radiologist. 7th ed. Philadelphia, PA: Lippincott Williams & Wilkins; 2012. p. 86-103.
20. Bindra RS, Crosby ME, Glazer PM. Regulation of DNA repair in hypoxic cancer cells. Cancer Metastasis Rev 2007;26:249-60.
21. Park HJ, Griffin RJ, Hui S, Levitt SH, Song CW. Radiation-induced vascular damage in tumors: implications of vascular damage in ablative hypofractionated radiotherapy (SBRT and SRS). Radiat Res 2012;177:311-27.
22. Butterworth KT, Coulter JA, Jain S, et al. Evaluation of cytotoxicity and radiation enhancement using 1.9 nm gold particles: potential application for cancer therapy. Nanotechnology 2010;21:295101.
23. Butterworth KT. Radiosensitization by gold nanoparticles: effective at megavoltage energies and potential role of oxidative stress. Transl Cancer Res 2013;2:269-79.
24. Misawa M, Takahashi J. Generation of reactive oxygen species induced by gold nanoparticles under x-ray and UV Irradiations. Nanomedicine 2011;7:604-14.
25. Ngwa W, Kumar R, Sridhar S, et al. Targeted radiotherapy with gold nanoparticles: current status and future perspectives. Nanomedicine (Lond) 2014;9:1063-82.
26. Hagtvet E, Roe K, Olsen DR. Liposomal doxorubicin improves radiotherapy response in hypoxic prostate cancer xenografts. Radiat Oncol 2011;6:135.